

RESEARCH

Open Access



# Comparative study of brain functional imaging of brain in patients with mild to moderate Alzheimer's disease based on functional near infrared spectroscopy

Zhen Yang<sup>1</sup>, Li Liu<sup>2</sup>, Tao You<sup>1</sup>, Lingling Wang<sup>1</sup>, Fang Yi<sup>3</sup>, Yu Jiang<sup>2</sup> and Ying Zhou<sup>2\*</sup>

## Abstract

**Objective** Based on the near-infrared functional brain imaging system, this research studied the hemoglobin concentration signal in resting state and task state. The purpose of this research was to analyze the activated brain regions and functional connections by exploring the changes in hemoglobin concentration and the differences in brain network functional connections between healthy people and mild to moderate AD patients. So as to identify the cognitive dysfunction of patients at an early stage. By accurately locating the area of cognitive impairment in patients, it provides a basis for precise neural regulation of physical therapy.

**Methods** Patients who came to our hospital from January 2022 to December 2022 were recruited and selected according to the exclusion criteria. After receiving their informed consent, MMSE scale examination and near-infrared brain function imaging examination were performed in a relatively quiet environment.

**Result** A total of 24 subjects were included in this study, including 7 in the control group (age:  $72.57 \pm 7.19$ ) and 17 (age:  $76.88 \pm 9.29$ ) in the AD group. The average cognitive scores were ( $28.00 \pm 1.16$ ), ( $19.24 \pm 4.89$ ), respectively. There were no statistically significant differences in gender, years of education, age, and past medical history between the AD group and the control group ( $P > 0.05$ ). In the verbal fluency test (VFT) task, there was a significant difference in the activation values of the two groups in channels 01, 06, 07, 09, 13, 14, 15, 16, 19, 21, 22, 23, 27, 29, 31, 35, 38, 40, 43, 44, 45, 51, and 52II ( $p < 0.05$ ), and the activation values of the normal group were greater than those of the AD group. There was a significant difference in the mean oxygenated hemoglobin concentration in channels 01, 07, 15, 16, 21, 22, 23, 31, 35, 40, 41, 44, and 48 ( $p < 0.05$ ), and the average oxygenated hemoglobin concentration in the AD group was lower than that in the normal group. There was no significant difference in activation speed between the two groups. In the resting state, the number of total network edges, DLPFC-L to PreM and SMC-L, DLPFC-L to FEF-L, DLPFC-L to DLPFC-L, FPA-L to PreM and SMC-L, FPA-L to FPA-L, FPA-R to FPA-L, DLPFC-L to DLPFC-R, FEF-R to PreM and There was a statistically significant difference in the number of network edges in SMC-L ( $p < 0.05$ ). Among the different groups, the number of network edges in the AD group was smaller than that in the normal group. Correlation analysis showed that T14, T31, T16, T23, T27, M16, M22, M41 (T: represents activation value, M: represents

\*Correspondence:

Ying Zhou  
1007866422@qq.com

Full list of author information is available at the end of the article



© The Author(s) 2024. **Open Access** This article is licensed under a Creative Commons Attribution-NonCommercial-NoDerivatives 4.0 International License, which permits any non-commercial use, sharing, distribution and reproduction in any medium or format, as long as you give appropriate credit to the original author(s) and the source, provide a link to the Creative Commons licence, and indicate if you modified the licensed material. You do not have permission under this licence to share adapted material derived from this article or parts of it. The images or other third party material in this article are included in the article's Creative Commons licence, unless indicated otherwise in a credit line to the material. If material is not included in the article's Creative Commons licence and your intended use is not permitted by statutory regulation or exceeds the permitted use, you will need to obtain permission directly from the copyright holder. To view a copy of this licence, visit <http://creativecommons.org/licenses/by-nc-nd/4.0/>.

mean hemoglobin concentration, and number represents channel number). There was a positive correlation between the total number of network edges, DLPFC-L to PreM and SMC-L, DLPFC-L to DLPFC-L, FPA-L to PreM and SMC-L, FPA-L to FPA-L, DLPFC-L to DLPFC-R, FEF-R to PreM and SMC-L, and MMSE scores ( $p < 0.05$ ).

**Discussion** In this study, we found hemodynamic changes in the prefrontal lobes of AD patients under the VFT task, and the decrease in the functional connectivity of the prefrontal brain network in AD patients in the resting state, and these changes were associated with cognitive decline in patients. Our findings suggest that fNIRS may be used as a tool for future clinical screening for cognitive impairment, and may also be used to develop personalized preventive measures and treatment plans through accurate assessment.

**Keywords** Alzheimer's disease(AD), Functional near infrared spectroscopy(fNIRS), Verbal fluency test (VFT), Dorsolateral prefrontal cortex (DLPFC)

## Introduction

Alzheimer's disease (AD) is a chronic neurodegenerative disease. The number of case is expected to reach 115 million by 2050 [1]. Clinically, AD is typically characterized by impaired recent memory, which gradually involves impairments in other cognitive function, such as speech, orientation, judgment, executive function and behavioral changes, and interfere with activities of daily living [2], with or without psychobehavioral abnormalities. The onset of AD is hidden and slowly progresses, and the early stage is dominated by recent memory decline, which is easy to be ignored as normal aging. In fact, the pathological changes of AD have occurred for many years before the obvious clinical symptoms of AD. Therefore, the clinical diagnosis of AD lags far behind the occurrence and development of AD. Although, Amyloid PET and Cerebral spinal fluid(CSF) A $\beta$ 42 measurement has been put into practical use in the stage of MCI, it is too expensive to carry out on a large scale in the clinic. In addition, the treatment of AD is still a worldwide problem, and the efficacy of drug therapy is limited. The determination of non-drug therapy (cognitive training, transcranial magnetic stimulation, electrical stimulation, etc.) requires a quantitative assessment of the brain function of patients, so as to provide guidance for determining and optimizing the treatment plan.

Currently, community-based autopsy studies indicate that vascular alterations are present in >50% of clinically diagnosed cases of AD. Large-scale multifactor analysis of neuroimaging images of Alzheimer's disease has shown that vascular dysregulation is an early and initial pathological event of AD and is associated with cognitive decline [3]. Neurons, astrocytes, microglia, endothelial cells, pericytes, basement membrane, and extracellular matrix work together in the brain to form the neurovascular unit (NVU), which regulates neurovascular coupling and thus regulates cerebral blood flow (CBF) through the brain [4]. Damage to neurovascular units causes a decrease in brain CBE, especially in brain regions involved in cognition, such as the hippocampus, entorhinal cortex, amygdala, and anterior cingulate gyrus, and

is observed in the preclinical stage of the disease [5]. The first evidence that amyloid changes cerebral vascular endothelial function in vivo was proposed by Zhang et al. The study observed cerebral vascular reactivity of AD mice overexpressing APP by applying endothelial-dependent tube dilator acetylcholine, and found that the cerebral cortex CBF of AD mice was reduced compared with that of normal mice. It suggests that the cerebrovascular action of metabolically derived peptides of Amyloid precursor protein (APP) may play a role in the pathogenesis of APP, and this phenomenon occurs before amyloid deposition or cognitive dysfunction [6]. There were also studies using exogenous A $\beta$ 40 to observe cerebral cortical CBF of APP transgenic mice, and it was found that A $\beta$ 40 (but not A $\beta$ 42) could reduce cerebral cortical CBF by inducing cerebral arteriole vasoconstriction, which proved A $\beta$  to have a direct impact on cerebral vessels [7]. These studies demonstrate that A $\beta$  affects brain circulation by reducing cerebral perfusion, further confirming that vascular dysfunction is an early manifestation of AB accumulation, and by identifying vascular dysfunction, we can help identify potential dementia risk in patients as early as possible.

Over the past 20 years, the introduction of functional Near-infrared spectroscopy (fNIRS) into the field of neuroscience has created new opportunities to study human brain function. fNIRS can monitor the dynamic changes of cerebral blood flow in patients in real time (with moderate time and fine spatial resolution) with relatively low cost, no radiation, portability, and very low motion sensitivity [8].

Blood circulation and brain function are interrelated through neurovascular coupling, also known as hemodynamic responses. When any area of our brain is activated, the neurons in that area need energy. This energy is provided by glucose metabolism, which requires oxygen, which is transported to the region through the Oxy-Hb[45]. Therefore, increasing amounts of Oxy-Hb or decreasing amounts of Deoxy-Hb indirectly suggest brain cell activation [9, 10]. Based on the Beer-Lambert law, fNIRS can easily and noninvasively measure changes in

hemoglobin concentration on the brain surface [11, 12]. This information can reflect changes in blood oxygen levels in the cerebral cortex to assess brain activity [13]. As a new generation of functional brain imaging technology, fNIRS is used to identify changes in cerebral hemodynamic characteristics of patients to study disease-related brain functional states and brain network functional connections [46]. In clinical practice, this technology is used to quantitatively assess brain function of patients, providing a favorable means for early warning of AD patients and providing guidance for personalized and precise treatment, which can improve treatment effectiveness and efficiency. The purpose of this study was to investigate the activated brain regions and functional connections by observing the changes of hemoglobin in resting state and task state of subjects and comparing the differences in hemoglobin concentration and functional connections of brain networks between mild to moderate AD subjects and cognitively normal control subjects. fNIRS was used to detect the activation of each brain functional region and the network connection status, so as to provide basis for early recognition of cognitive dysfunction and precise neural regulation for treatment.

## Method

### Study object and group

AD patients who came to Changsha First Hospital from January 2022 to December 2022 were selected, and the inclusion criteria were: (1) Patients > 60 years of age, (2) probable diagnosis of AD (International Classification of Diseases 10th Edition of the World Health Organization (ICD-10)), (3) MMSE score of 11–26, with more than 6 years of education, and (5) CDR score of 1–2, volunteered to participate in this study. Exclusion criteria: (1) no self-care ability, (2) other diseases affecting cognitive function (vascular dementia, Parkinson's disease, frontotemporal dementia, epilepsy, severe anemia, severe liver and kidney insufficiency, etc.), (3) refused to participate in this experiment, (4) could not complete the fNIRS examination, (5) suffered from depression, (6) Head MRI showed Fazekas scale (Appendix 2)  $\geq 2$ . Recruit a matching control group based on the basic situation of the enrolled. Before fNIRS monitoring, all subjects were evaluated by Mini-Mental State Examination (MMSE), which was divided into two groups: control group (subjects with MMSE > 26 points were considered to have normal cognition) and AD group (with MMSE < 26 points, in line with the sodium standard).

The qualified personnel are investigated, and the unified questionnaire is adopted by the professionally trained investigators, and the face-to-face questionnaire survey is conducted after the informed consent of the surveyed subjects (Appendix). The content includes general demographic information (gender, age, education,

retirement years, pre-retirement employment, marital status, way of living, handedness, medical history) and lifestyle habits (smoking, alcohol consumption).

### General data collection

The general data include age, sex, education, handedness, marital status, past illness, and life after retirement. Previous medical history: Chronic medical history, including hypertension, diabetes, hyperlipidemia, cardiovascular and cerebrovascular diseases, was 0 for those without chronic medical history, 1 for those with one chronic medical history, and 2 for those with two chronic medical histories or more.

### fNIRS tool

A 53-channel fNIRS device ((BS-7000, Wuhan Znion Technology Co, Ltd, China) was used to measure the three types of relative concentration changes of Oxy-Hb, Deoxy-Hb, and Total-Hb by near-infrared light of a specific wavelength. The instrument has 16 pairs of emission and detector probes. The wavelengths of light emitted are 690 nm and 830 nm, and the frequency is 15.625 Hz. The distance between each emitter and detector is 2.9–3.1 cm. The area between the emitter and detector probes consists of a channel. Each probe was positioned on the scalp of the forehead. The optode arrangement is shown in Fig. 1 and is based on the 10/20 System of Electrode Placement method, which is also commonly used in EEGs. The numbers represent remitter probes, with the letters representing detector probes [14].

A total of 16 pairs of optodes and 53 channels. The numbers represent remitter probes, with the letters representing detector probes. In Fig. 2, Channels 01 (ch01), ch04, ch10, ch40, ch47 and ch52 belong to the Pre-Motor and Supplementary Motor Cortex (PreM and SMC). Ch02, ch03, ch05, ch07, ch08, ch13, ch44, ch46, ch49, ch50, ch51 and ch53 belong to the Broca's area. Ch06, ch11, ch14, ch17, ch18, ch20, ch25, ch31, ch32, ch34, ch39, ch42 and ch45 belong to the dorsolateral prefrontal cortex (DLPFC). Ch12, ch24, ch26, ch38 belong to the frontal eye fields (FEF). Ch09, ch15, ch16, ch19, ch21, ch22, ch23, ch27, ch28, ch29, ch30, ch33, ch35, ch36, ch37, ch41, ch43 and ch48 belong to the frontal pole area (FPA). All tasks are completed in the morning (8am – 12pm), first completing the resting state task and then completing the VFT task.

### MMSE

An initial assessment of cognitive function, currently the most widely used scale, includes orientation (10 points), immediate memory (3 points), attention and numeracy (5 points), recall (3 points), and verbal ability (9 points), out of a possible 30 points.

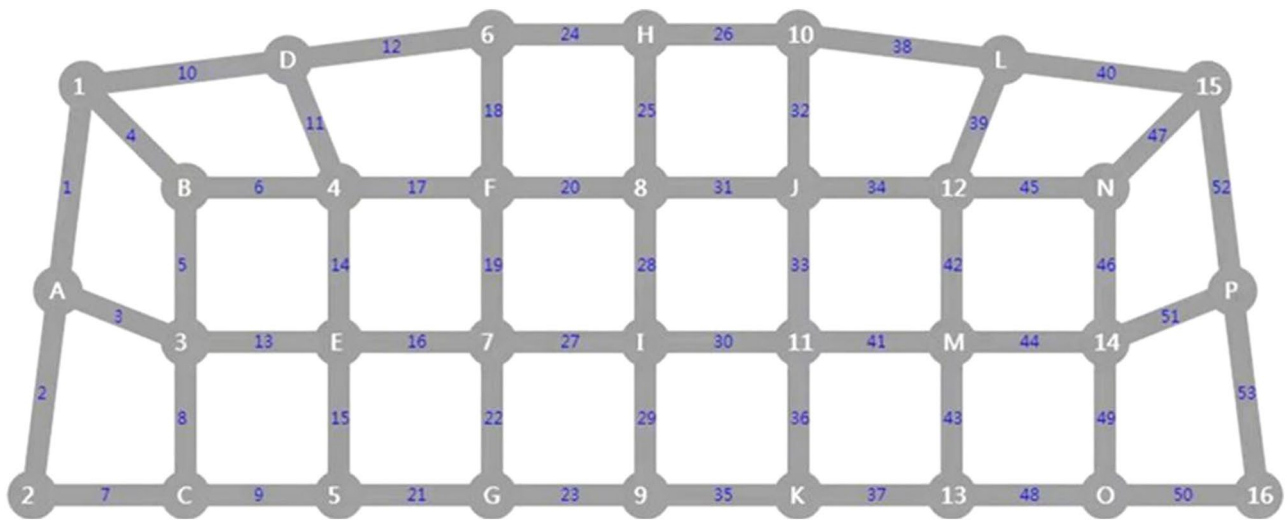


**Fig. 1** Space arrangement of transmitting and receiving probes

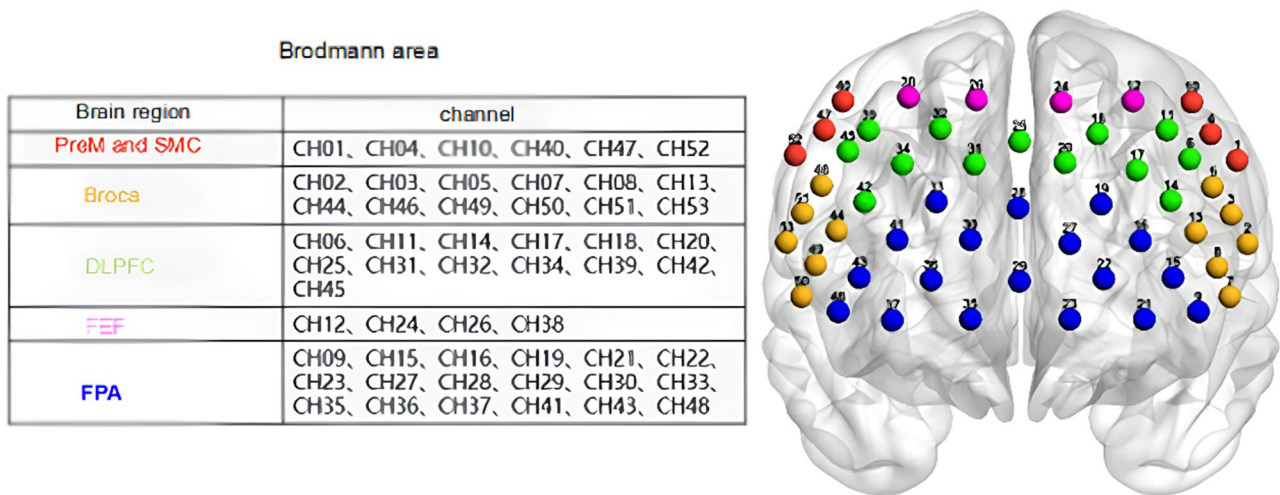


**Fig. 2** Spatial distribution of each channel and division of brain regions

**Resting data acquisition**

The patient was seated and rested for 5 min while wearing the fNIRS device. The patient was asked to relax, look at the black cross 50 cm in front, and keep the head as stable as possible. The original fNIRS data of the patient was collected for 150 s [15].

**Verbal fluency test (VFT) data acquisition**

The patient was seated and rested for 5 min while wearing the fNIRS device. Before the task began, the patient followed the voice prompt to count for 30 s. Then complete 3 groups of tasks (please name a variety of vegetables, please name a variety of fruits, please name a variety of animals), each group of tasks lasts 20 s. Then continue to followed the voice prompt to count for 60 s [16].

**fNIRS data preprocessing**

fNIRS signal is processed by MATLAB2014b. The original fNIRS data were converted to the concentration changes of Oxy-Hb and Deoxy-Hb using the modified Beer-Lambert Law [17]. Physiological noise (heart noise ~1 Hz, respiratory noise ~0.25 Hz, Mayer signal ~0.1 Hz) and mechanical noise were filtered by band-pass filter with cut-off frequency range of 0.005 Hz ~0.1 Hz, and motion artifacts were identified and removed. The data is then split into task time and resting time. Baseline correction was performed for each subject by subtracting average resting state data (30 s before task start and 60 s after task completion) from the task data [18]. For VFT tasks, the signal of each channel is collected for further analysis of the characteristics. The characteristics selected were activation value(T value), slope, and average oxygenated hemoglobin concentration [19, 20]. Because Oxy-Hb has

a better signal-to-noise ratio, it can reflect task-related cortical activation more directly than Deoxy-Hb. Therefore, this study focused on the changes of Oxy-Hb. The standard Hemodynamic response function (HRF) in this study was generated by convolution of the stimulation mode (i.e., the 60-second task cycle and the 90-second rest cycle) with the typical hemodynamic response function composed of two gamma functions [21]. The activation value (T value) is defined as the ratio of the weight factor (when the measurement data is linearly fitted to the HRF) to the standard error [22]. The meaning of the T-value in this study is conceptually the same as in the fMRI field, where a high T-value indicates a strong correlation between the signal and HRF.

By measuring the difference in mean oxygen and hemoglobin values between the task and the pre-task phase, the mean changes in oxygenated hemoglobin concentrations across 53 channels were calculated. The mean oxygenated hemoglobin value is the average over the entire test time window. The slope indicates the speed of activation.

For the resting state data, the correlation of hemoglobin changes among different channels was calculated using NIRS-KIT [23] software, and the R-value was calculated by Spearman correlation analysis.  $r \geq 0.5$  was defined as a connection between channels, and the number of connecting edges between each functional zone was analyzed, and the strength of functional connections of each functional zone in the resting state was represented by the size of the edge number. Use BrainNets [24] to make correlation matrix plots. On the basis of correlation matrix, channels are taken as network nodes and the connections between channels are taken as network edges. By calculating the number of network edges of correlation coefficient  $r \geq 0.5$ , the strength of each functional connection area is further analyzed. The number of edges of networks with intra-hemispheric connections and inter-hemispheric connections, as well as short connections (connections between each functional area in the hemisphere and its own connections and connections between other functional areas) and long connections

(connections between each functional area and functional areas in the other hemisphere) were counted respectively.

### Statistical method

SPSS27.0 statistical software was used for data processing. Normal test was performed on the measurement data. The measurement data conforming to normal distribution were expressed as  $(X \pm s)$ , and the two independent samples T-test was used for comparison between groups. The measurement data that did not conform to the normal distribution were represented by M (Q1, Q3), and the measurement data of the Mann-Whitney U test line were represented by  $(x \pm s)$  for inter-group comparison. Counting data were expressed as relative numbers, and Chi-square test was used for comparison between groups. Spearman correlation analysis was used, and  $p < 0.05$  indicated statistically significant difference between the two groups.

## Result

### Demographic data

A total of 24 subjects were included in this study, including 7 (age:  $72.57 \pm 7.19$ ) in the control group and 17 (age:  $76.88 \pm 9.29$ ) in the AD group. All patients were right-handed. There was no significant difference between AD group and control group in gender, years of education and previous disease ( $P > 0.05$ ). The MMSE score of the control group was higher than that of the AD group, and the difference was statistically significant ( $P < 0.05$ ) (Table 1).

### Task state data analysis

#### Comparison between activation values (t values)

In the VFT task, the hemoglobin concentration in each channel with time, as shown in Fig. 3. The activation values of each channel are shown in Table 2. Among them, the premotor cortex and supplementary motor area (CH01, 40, 52), dorsolateral prefrontal lobe (CH06, 14, 31, 45), Broca area (CH51, 07, 44, 13), and frontal polar area (CH09, 15, 16, 19, 21, 22, 23, 27, 17, 13). The activation values of 29, 35, 43) and frontal eye field (CH48) were statistically significant ( $p < 0.05$ ), and the activation values of meaningful channels in AD group were all lower than those in control group. The activation diagrams of the two groups of channels are shown in Figs. 4 and 5.

#### Comparison of average hemoglobin concentrations

In the VFT task, the hemoglobin concentration of each channel is shown in Table 3. Among them, the premotor cortex and supplementary motor area (CH01, CH40), Broca area (CH07, CH44), frontal polar area (CH15, CH16, CH21, CH22, CH23, CH35, CH41, CH48), and dorsolateral prefrontal lobe (CH31) were significantly

**Table 1** Basic information

Clinical data	Control group (n = 7)	AD group (n = 17)	T(x2)	P
Year	$72.57 \pm 7.19$	$76.88 \pm 9.29$	1.095	0.285
Gender	Male 3(42.9%) Female 4(33.3%)	9(52.9%) 8(66.7%)	0.202	0.653
MMSE*	$28.00 \pm 1.16^*$	$19.24 \pm 4.89$	-4.632	<0.01
Years of schooling	$10.43 \pm 3.21$	$12.24 \pm 3.09$	1.288	0.211
Anamnesis	03(42.8%) 12(28.6%) 22(28.6%)	6(35.3%) 7(41.2%) 4(23.5%)	0.336	0.845

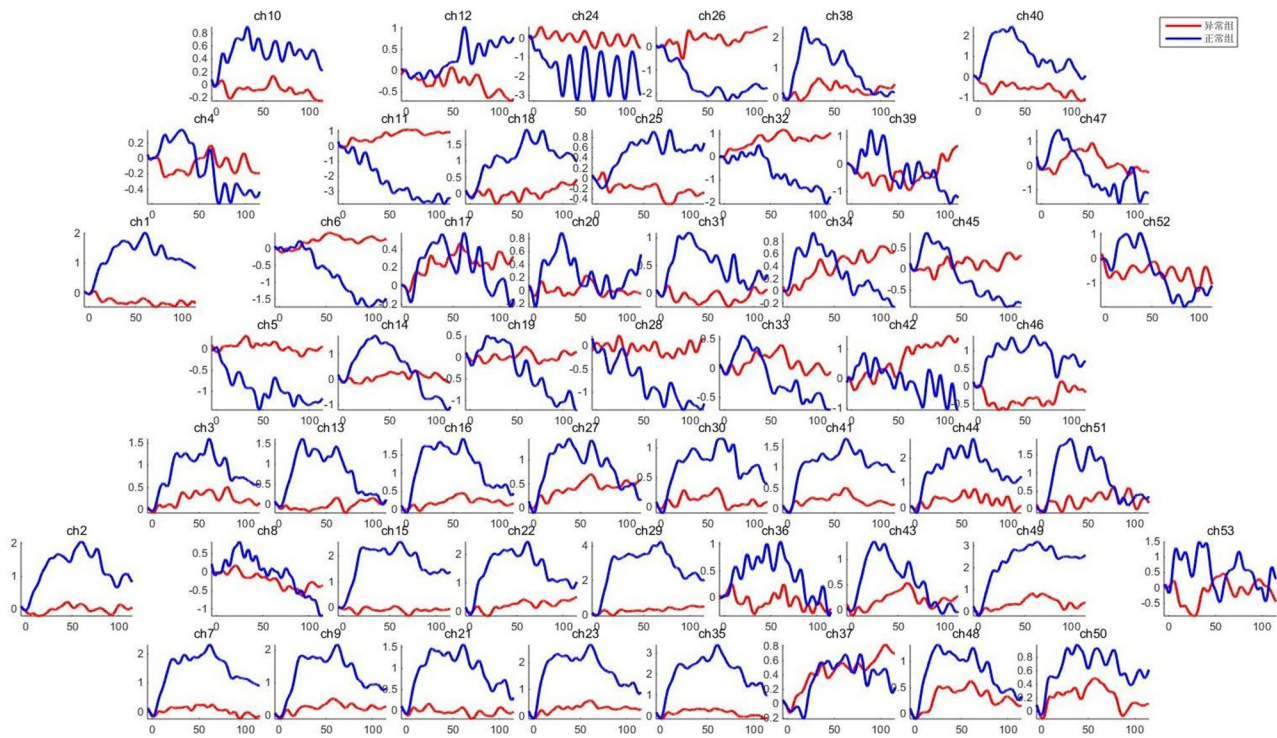


**Fig. 3** Changes in subject hemoglobin during the VFT task in both groups. The abscissa is time and the ordinate is hemoglobin concentration.(blue-Control group, red- AD group)

**Table 2** The value of each channel activation between the two groups(t value)

Brain regions	Channels	Control group	AD group	P value
PreM and SMC	Ch01*	1.62±0.94	-0.16±0.34	0.033
	Ch40*	2.19±1.67	-0.82±0.40	0.002
	Ch52*	1.81±1.95	0.58±0.51	0.019
DLPFC	Ch06*	1.78±1.00	0.48±0.32	0.027
	Ch14*	2.74±1.33	-0.59±0.29	0.0003
	Ch31*	2.21±0.66	0.03±0.26	0.007
	Ch45*	2.46±0.70	0.09±0.50	0.020
Broca	Ch51*	3.21±0.91	-0.57±0.36	0.0001
	Ch07*	3.09±0.64	2.06±0.26	0.003
	Ch44*	2.57±0.89	0.61±0.71	0.042
FPA	Ch13*	1.84±1.18	-0.78±0.40	0.010
	Ch09*	1.88±1.02	0.69±0.35	0.025
	Ch15*	1.65±1.40	0.12±0.46	0.033
	Ch16*	2.44±1.02	0.66±0.26	0.002
	Ch19*	2.31±0.79	0.64±0.25	0.005
	Ch21*	1.91±0.86	0.54±0.36	0.031
	Ch22*	1.86±1.30	-0.42±0.33	0.009
	Ch23*	2.68±1.00	1.06±0.33	0.002
	Ch27*	2.40±0.63	1.04±0.23	0.008
	Ch29*	1.38±2.46	-0.45±0.25	0.036
FEF	Ch35*	1.90±1.37	1.76±0.42	0.038
	Ch43*	2.11±0.98	1.37±0.29	0.015
	Ch38*	2.77±1.21	0.74±1.03	0.041

different ( $p < 0.05$ ). In addition, the mean hemoglobin concentration in AD group was lower than that in control group in statistically significant channels. The brain regions with hemoglobin concentrations in the two groups are shown in Fig. 6.

**Comparison between the slopes of each channel in the two groups**

In the VFT task, we selected 2–7 s after the task started to calculate the slope. The slope of each channel is shown in Table 4. There were significant differences in frontal polar region (CH16), premotor cortex and supplementary motor cortex (CH40) ( $p < 0.05$ ). The slope of the channels in the AD group was lower than that in the control group. Figure 7 shows the slope of each brain area in the two groups.

**Analysis of resting state result**

For the resting state data, this study calculated the correlation between the changes in oxy-hemoglobin concentration of each channel (Fig. 8 shows the functional connection matrix of the two groups), and made the functional connection matrix between each channel according to the magnitude of the correlation, and Fig. 9 shows the connection of the functional area.

As can be seen from Table 5, there were statistically significant differences in the network edge number of

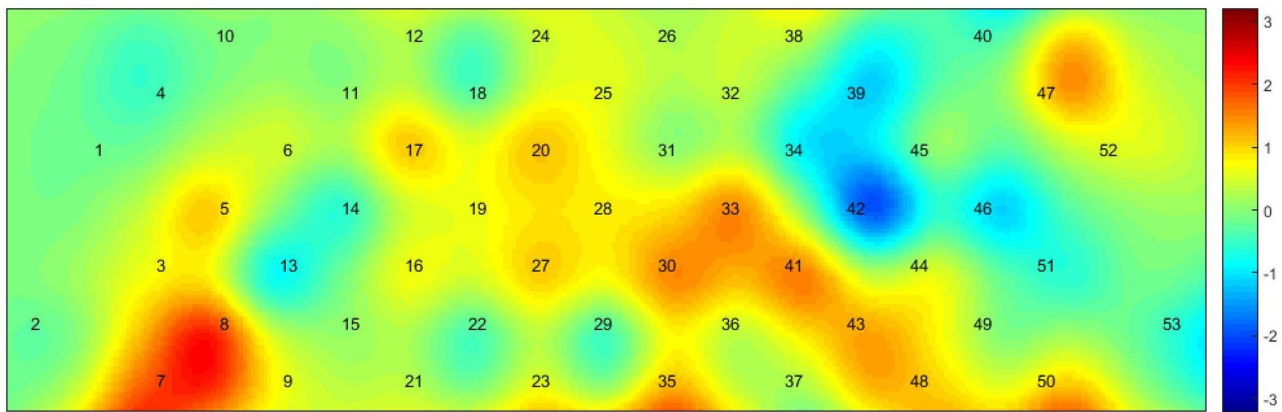


**Fig. 4** Activation diagram of each channel of the AD group

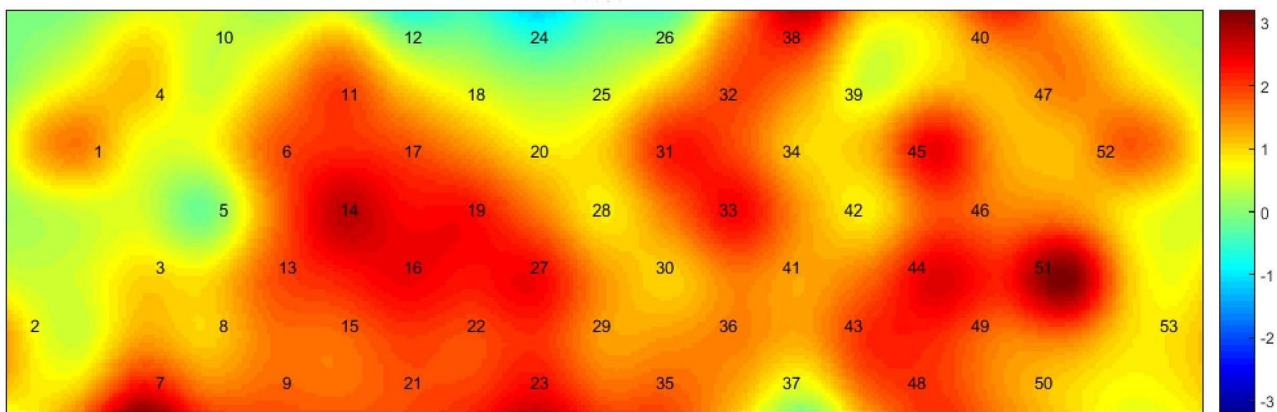


**figure. 5** Activation diagram of each channel of the control group

**Table 3** Average hemoglobin protein for each channel between the two groups

Brain egions	Channel	Control group	AD group	P value
PreM and SMC	Ch01*	1.28±1.55	0.23±1.01	0.009
	Ch40*	1.69±2.03	0.47±1.36	0.005
Broca	Ch07*	1.50±0.97	0.12±0.50	0.008
	Ch44*	1.65±0.69	0.31±0.86	0.001
FPA	Ch15*	1.83±2.10	0.06±0.98	0.006
	Ch16*	1.43±1.21	0.19±0.53	0.035
	Ch21*	1.10±1.12	0.002±0.36	0.013
	Ch22*	1.67±1.12	0.14±0.59	0.018
	Ch23*	0.93±1.44	0.26±0.80	0.001
	Ch35*	2.19±1.92	0.23±0.71	0.039
	Ch41*	1.02±0.80	0.22±0.56	0.010
	Ch48*	0.96±0.78	0.34±0.62	0.047
DLPFC	Ch31*	0.72±0.82	-0.07±0.37	0.044

the total, DLPFC-L to PreM and SMC-L, DLPFC-L to FEF-L, .

DLPFC-L to DLPFC-L, FPA-L to PreM and SMC-L, FPA-L to FPA-L, FPA-R to FPA-L, DLPFC-L to DLPFC-R, FEF-R to PreM and SMC-L( $p<0.05$ ). Among

the different groups, the mean value of AD group was lower than of control group.

**Correlation analysis**

For data at rest state and VFT task, correlation analysis is shown in Tables 6 and 7. It is found in the table that the total number of network edges at rest ( $r=0.431, p<0.05$ ), DLPFC-L to PreM and SMC-L ( $R=0.521, p<0.05$ ), DLPFC-L to DLPFC-L ( $r=0.590, p<0.05$ ), FPA-L to PreM and SMC-L ( $r=0.406, p<0.05$ ), FPA-L to FPA-L ( $r=0.415, p<0.05$ ), DLPFC-L to DLPFC-R ( $r=0.482.05$ ), FEF-R to PreM and SMC-L ( $r=0.589, p<0.05$ ) were positively correlated with MMSE score. The MMSE scale was divided into orientation (10 points), memory (6 points), including (immediate memory and recall), attention and calculation (5 points), and language ability (9 points). The hierarchical MMSE scores between the two groups were shown in Table 8. Pearson correlation analysis was conducted between the data with differences extracted from the above results and different cognitive domain scores, and the results were shown in Tables 9, 10.

It can be seen from the table that DLPFC-L to PreM and SMC-L, DLPFC-L to DLPFC-L, FPA-L to PreM

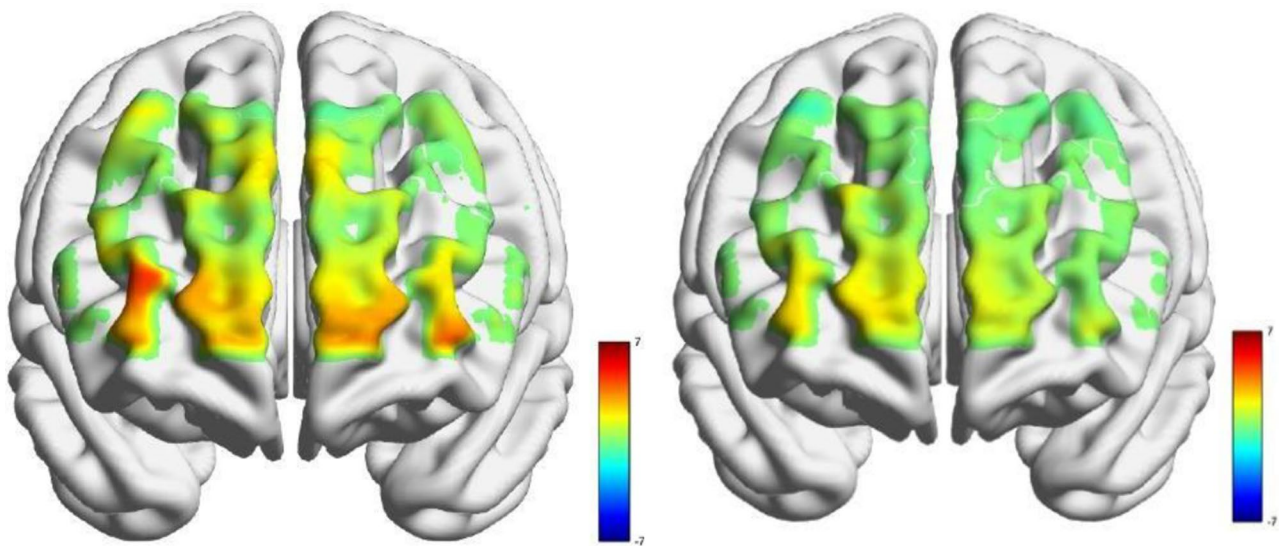


**Fig. 6** The mean hemoglobin concentration of the control group is shown on the left, and the hemoglobin concentration of the AD group is shown on the right

**Table 4** The slope of each channel between the two groups

Brain regions	Channel	Control group	AD group	P value
FPA	Ch16*	0.14±0.12	0.03±0.07	0.048
PreM and SMC	Ch40*	0.19±0.24	-0.01±0.13	0.010

and SMC-L, DLPFC-L to DLPFC-R were positively correlated with orientation score. DLPFC-L to PreM and SMC-L, DLPFC-L to DLPFC-L, FEF-R to PreM and SMC-L were positively correlated with memory scores. DLPFC-L to DLPFC-L, FEF-R to PreM and SMC-L were positively correlated with attention and numeracy. The total total number of network edges at rest, DLPFC-L to PreM and SMC-L, DLPFC-L to FEF-L, DLPFC-L to

DLPFC-L, FPA-L to PreM and SMC-L, FPA-L to FPA-L, DLPFC-L to DLPFC-R, FEF-R to PreM and SMC-L were positively correlated with language ability Tables 11 and 12.

**Discussion**

In this study, verbal fluency test (VFT) is used to assess the cognitive functions of patients, which is one of the commonly used methods to assess the cognitive functions of patients [25]. VFT tasks can be used to measure a variety of cognitive abilities, such as executive function, processing speed, word retrieval, and memory [26]. Most studies have focused on extracting the mean and

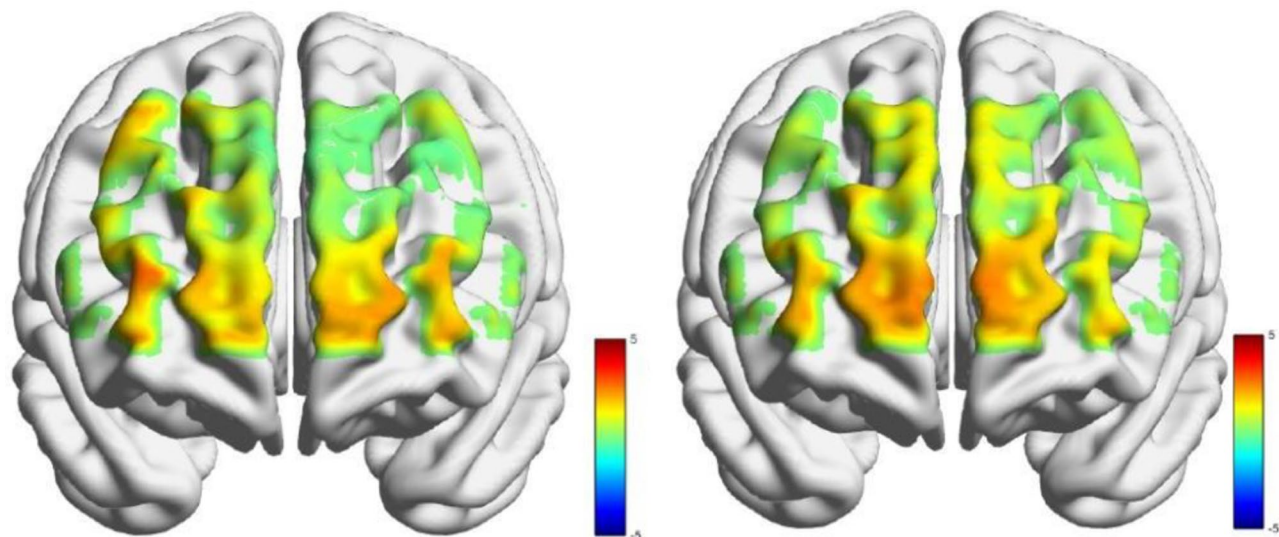


**Fig. 7** The left figure is a schematic diagram of the slope of each channel in the control group, and the right is a schematic diagram of the AD group

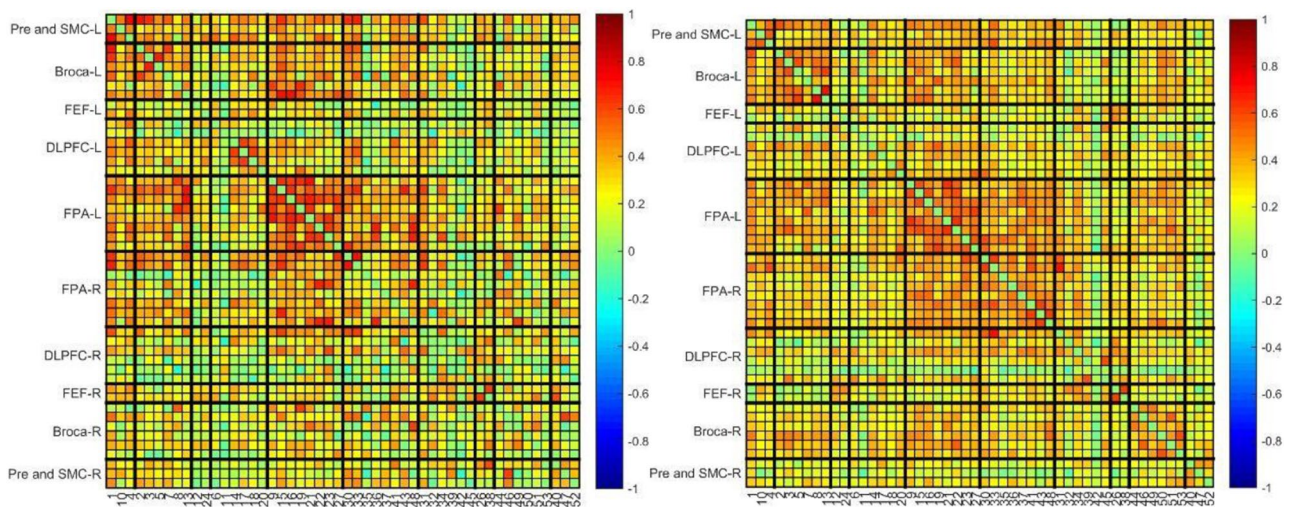


**Fig. 8** On the left is the control group functional connectivity matrix, and on the right is the AD group functional connectivity matrix

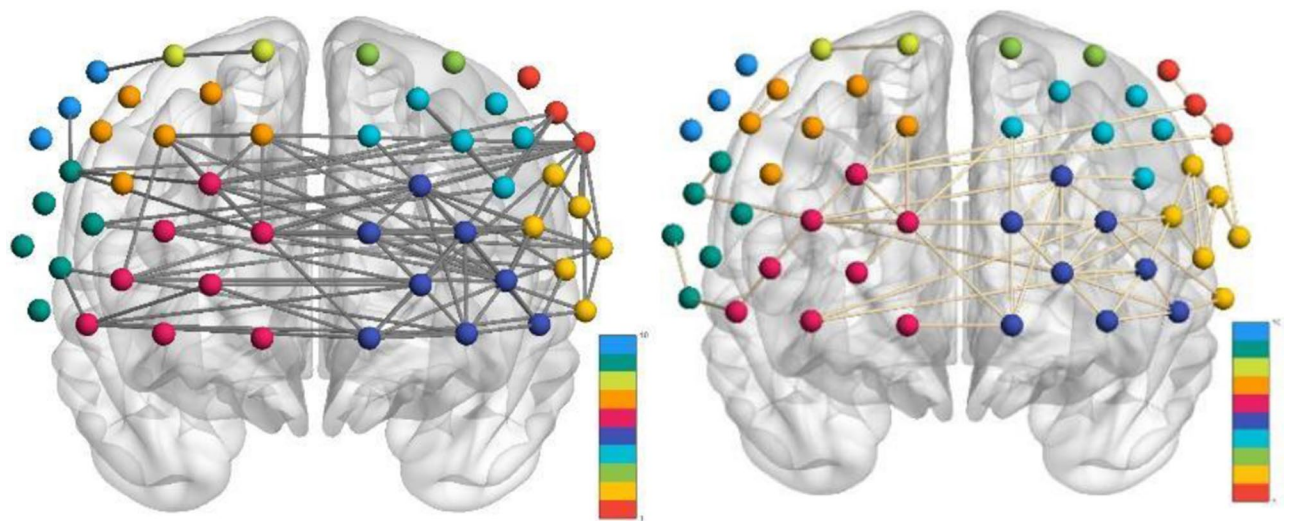


**Fig. 9** Schematic diagram of the connection of each functional area, with the control group on the left and the AD group on the right. Different colors represent different brain regions

**Table 5** Comparison of functional connectivity strength of various brain regions in the resting state

	Control group	AD group	P value
Total Network Edges*	477.14 ± 245.25	257.76 ± 130.38	0.090
DLPFC-L to PreM and SMC-L*	9.43 ± 3.95	4.35 ± 4.27	0.013
DLPFC-L to FEF-L*	5.29 ± 3.45	2.76 ± 1.89	0.030
DLPFC-L to DLPFC-L*	5.57 ± 2.70	2.82 ± 2.43	0.023
FPA-L to PreM and SMC-L*	13.71 ± 7.99	6.35 ± 4.80	0.010
FPA-L to FPA-L*	21.43 ± 5.77	11.29 ± 7.10	0.030
FPA-R to FPA-L*	37.00 ± 17.39	22.29 ± 11.76	0.024
DLPFC-L to DLPFC-R*	11.14 ± 6.77	5.06 ± 3.46	0.008
FEF-R to PreM and SMC-L*	3.57 ± 2.30	0.88 ± 1.21	0.010

peak values of Oxy-Hb to assess subjects’ brain activity, but this study not only studied the mean values of Oxy-Hb, but also extracted various other features that reflect the activation of the prefrontal cortex, thus reflecting the activation state of the brain.

In this study, by measuring fNIRS signals from the frontal region during the VFT task, this study was able to identify different Oxy-Hb response patterns in the two study groups to provide precise targeting for future neuroregulatory therapy. On the other hand, the association of fNIRS-derived indicators (including activation, mean hemoglobin concentration, and functional connectivity of resting brain networks) with clinical scores suggests that fNIRS can be used as a clinical routine tool to assess cognitive function, monitor disease development, and evaluate rehabilitation. VFT task performance in AD

**Table 6** Correlation analysis of VFT task data with MMSE score

Brain regions	Channel	Correlation coefficient	P value
FPA	M15	0.299	0.155
	M16*	0.475	0.019
	M21	0.323	0.124
	M22*	0.434	0.034
	M23*	0.497	0.014
	M35*	0.475	0.019
	M41*	0.527	0.008
	M48	0.462	0.462
DLPFC	M31	0.383	0.065
	T6	0.290	0.169
	T14*	0.481	0.017
	T31*	0.431	0.036
	T45	0.319	0.059
FPA	T9	0.237	0.264
	T15	0.226	0.288
	T16*	0.469	0.021
	T19	0.333	0.112
	T21	0.354	0.089
	T22	0.253	0.232
	T23*	0.530	0.008
	T27*	0.415	0.044
	T29	0.284	0.179
	T35	0.384	0.064
T43	0.351	0.092	

Note: T-Activation Value, M-mean hemoglobin concentration, The number represents the channel number

**Table 7** Correlation analysis of resting state data with MMSE score

	Correlation coefficient	P value
Total Network Edges	0.431	0.036
DLPFC-L to PreM and SMC-L	0.521	0.009
DLPFC-L to FEF-L	0.388	0.061
DLPFC-L to DLPFC-L	0.590	0.002
FPA-L to PreM and SMC-L	0.406	0.049
FPA-L to FPA-L	0.415	0.044
FPA-R to FPA-L	0.210	0.325
DLPFC-L to DLPFC-R	0.482	0.017
FEF-R to PreM and SMC-L	0.589	0.002

**Table 8** MMSE score for subjects in both groups

	Control group	AD group	P value
MMSE score	28.00 ± 1.16	19.24 ± 4.89	<0.001
Orientation	9.71 ± 0.49	7.29 ± 1.61	<0.001
Memory	4.57 ± 0.53	3.06 ± 1.30	0.007
Attention and calculation	5.43 ± 0.53	2.88 ± 1.41	<0.001
Language ability	8.29 ± 0.76	6.00 ± 1.28	<0.001

patients has been found to be associated with structural and functional changes in brain regions, including the medial and lateral temporal lobes, frontal regions such as the anterior cingulate, prefrontal cortex, superior and middle frontal gyrus, parietal, and parietal lobules [27].

**Table 9** Correlation analysis of resting data with language proficiency scores

	Correlation coefficient	P value
Total Network Edges	0.573	0.003
DLPFC-L to PreM and SMC-L	0.603	0.002
DLPFC-L to FEF-L	0.542	0.006
DLPFC-L to DLPFC-L	0.670	<0.001
FPA-L to PreM and SMC-L	0.471	0.020
FPA-L to FPA-L	0.542	0.006
DLPFC-L to DLPFC-R	0.631	<0.001
FEF-R to PreM and SMC-L	0.525	0.008

**Table 10** Correlation analysis of resting data with orientation

	Correlation coefficient	P value
DLPFC-L to PreM and SMC-L	0.479	0.018
DLPFC-L to DLPFC-L	0.551	0.005
FPA-L to PreM and SMC-L	0.406	0.049
DLPFC-L to DLPFC-R	0.425	0.038

**Table 11** Correlation analysis of resting data with attention and calculation

	Correlation coefficient	P value
DLPFC-L to DLPFC-L	0.424	0.039
FEF-R to PreM and SMC-L	0.480	0.018

**Table 12** Correlation analysis of resting data with memory

	Correlation coefficient	P value
DLPFC-L to PreM and SMC-L	0.477	0.019
DLPFC-L to DLPFC-L	0.500	0.013
FEF-R to PreM and SMC-L	0.607	0.002

This study focused on differences in patients' prefrontal cortex, which is the last structure to emerge and mature in phylogeny, and that is about 29% of the entire adult human cerebral cortex. The prefrontal cortex is a key brain region associated with many higher cognitive functions. For example, it plays a key role in the cognition of abstract rules, working memory, attention regulation, as well as in the planning and strategy of behavior, thinking and reasoning. Since the interaction between the prefrontal cortex and the hippocampus is critical for cognition and adaptive behavior, especially memory storage and consolidation [28]. Secondly, about 2/3 of the hippocampus Amun's corner 1 area and the hippocampal hypothalamus are linked to the medial prefrontal cortex [29]. Theoretically, the prefrontal cortex-hippocampus dysfunction is the root cause of various neurocognitive symptoms.

In this study, the frontal lobe was divided into the following 5 functional areas. The dorsolateral prefrontal cortex (DLPFC) has extensive connections with the sensory and motor cortex and is key to regulating attention, thinking, and action. The frontal polar area (FPA) is

mainly associated with mental activities (such as thinking, judgment, intelligence, emotion and memory) and muscle coordination. The Broca area is responsible for the processing of speech information and the production of speech. The premotor cortex and supplementary motor cortex (PreM and SMC) are responsible for controlling certain aspects of movement, including preparation for movement, sensory orientation during movement, spatial orientation, and partial movement involving the proximal and trunk muscles of the body, internal planning of movement, organization before and after the movement sequence, and coordination between the two sides of the body. Frontal eye field (FEF) is mainly related to the coordinated movement of both eyes. Since the PreM and SMC and Broca regions are susceptible to the influence of the subject's state (in the experiment, subject's involuntary body movement and speech), this study focuses on the brain regions (DLPFC and FPA) that play an important role in cognitive function.

#### **fNIRS as a tool for early identification of cognitive impairment**

This study found that there were differences in cerebral hemodynamic response between AD group and control group, and Oxy-Hb concentration was decreased in AD group. This is consistent with the findings of previous studies, which observed a decrease in Oxy-Hb concentration in the prefrontal lobe in patients with MCI and AD [30, 31]. Possible pathophysiological mechanisms of this finding are: on the one hand, when performing cognitive tasks, AD patients may have reduced local cerebral blood flow due to vascular dysfunction, which will lead to a delay in the decrease or increase of Oxy-Hb concentration shortly after the task begins. On the other hand, since AD-induced neurodegeneration may induce functional recombination, compensation of cerebral blood flow in other regions may be required to support the decline in brain function, leading to an increase in overall oxygen consumption [32].

Resting state functional connectivity represents the baseline neuronal activity of the human brain in the absence of external stimuli and identifies the presence of functionally different networks [33]. This theory is supported by fMRI [34]. This study found that the total brain network edge number in AD group was significantly lower than that in the control group, and the total brain network edge number represented the functional connection strength of the prefrontal network, suggesting a decline in the functional connection strength of the prefrontal network in AD group. Subregional observation showed that these functional connectivity declines were mainly concentrated in DLPFC and other brain areas and its own network connectivity, and FPA was positively correlated with other brain areas and its own network

connectivity, and it was positively correlated with MMSE score. This is consistent with previous studies. TongBoon Tang et al. analyzed the functional connectivity of brain networks in subjects with normal aging and mild AD, and found that the functional connectivity of prefrontal cortex in AD patients generally declined [35]. In these studies, the loss of connectivity may be due to an increase in beta-amyloid deposition [31, 36–38]. A PET-based study found scattered A $\beta$  deposits in the frontal, parietal, temporal, or occipital cortex (i.e. the neocortex) early in cognitive decline in AD. In this study, we found that the decreased connection strength of various brain functional areas in the prefrontal lobe was located on the left side, which may be related to the patients' right-handedness, which is still worth further exploration. It was found that the connection strength of DLPFC and other brain functional areas on the left and the connection strength of PFA with other brain functional areas were decreased. A systematic review of 36 related articles from the past 20 years showed that patients with MCI and AD had impaired functional connectivity of brain networks in the prefrontal cortex during resting states [39]. By detecting activation of prefrontal cortex in task state and functional connectivity of brain network in resting state, fNIRS may serve as a portable and reliable clinical detection tool for early identification of AD. The results of this study showed that there was no significant difference in the activation rate between the AD group and the control group, which may be due to the fact that a large number of microcirculation opened after the task began, which played a partial compensatory role in the early stage of the task. It should be noted that because fNIRS can only measure the hemodynamic response at the cortical surface (1–3 cm), it is not possible to study any potential pathological changes in the subcortical or deep structures, which may play an important role in the abnormal reduction and delay of the hemodynamic response in AD.

#### **fNIRS provides precise targeting for neuroregulatory therapies**

Because fNIRS can overcome some limitations of other traditional functional brain imaging techniques, it is more suitable for multiple acquisition in a real rehabilitation environment. In fact, this technology can be measured in a natural context, and the subject can blink, speak, and move appropriately during use, without causing undue discomfort to the subject, improving the subject's acceptance, and without interfering with diagnosis and treatment. In addition, fNIRS can operate in performing a variety of different tasks, such as motor, somatosensory, or cognitive tasks [9].

In this study, the prefrontal lobe was divided into 53 channels, and the activated brain regions and functional connectivity states were analyzed. It was found that the

network connectivity between DLPFC-L-DLPFC-L was correlated with various cognitive function scores. It may be related to the fact that DLPFC is an evolutionarily specific cortex of primates and plays a central role in cognitive processes. The DLPFC is believed to underlie the rich and complex nature of cognition in humans and other primates, and the DLPFC has extensive connections to other brain regions. The DLPFC is believed to underlie the rich and complex nature of cognition in humans and other primates, and the DLPFC has extensive connections to other brain regions [40]. A large number of studies based on repetitive transcranial magnetic stimulation in the treatment of cognitive impairment have found that cognition is improved after high-frequency stimulation of the left dorsolateral prefrontal cortex [41]. Therefore, the mechanism by which repetitive TMS therapy can improve patients' cognitive performance may be achieved by improving the functional connectivity of patients' brain networks. Studies have shown that NIRS can be used to assess the recovery of patients after stroke [42]. Therefore, fNIRS technology, by accurately mapping activation maps and functional connectivity maps of brain networks, may provide key sites related to cognition for non-invasive neuroregulatory therapy (transcranial magnetic stimulation therapy, direct current stimulation therapy, alternating current stimulation therapy, etc.). In addition, by understanding the relationship between functional recovery and hemodynamic pattern change after injury or during rehabilitation, we can judge the effect of neuroregulatory treatment, and provide a basis for formulating and optimizing treatment plan.

## Summary

To sum up, this study found prefrontal hemodynamic changes in AD patients under the VFT task, and the functional connectivity strength of prefrontal brain network decreased in AD patients in the resting state, and these changes were related to the cognitive decline of patients. fNIRS can extract complex and diverse variables for analysis, providing good specificity and sensitivity for early identification of AD. Our findings suggest that fNIRS may be used as a tool for future clinical screening for cognitive impairment, as well as for personalized prevention and treatment through precise assessment.

## Research deficiencies and prospects

There are several limitations to this study. First, these signals are not solely based on neuronal signals, but also include signals generated by scalp effects and physiological noise, and eliminating this effect should consider the use of multi-range probes and independent component analysis. In addition, due to the epidemic situation, the sample size is small, not comprehensive, and there is insufficient efficacy of the test, so it is necessary to

further expand the sample size to extract good specificity and sensitivity indicators for the early identification and precise neuroregulatory treatment of AD. With the development of fNIRS devices and the optimization of imaging algorithms, the research on functional connectivity of whole brain networks and the application of multimodal imaging technology can be realized in the future.

## Supplementary Information

The online version contains supplementary material available at <https://doi.org/10.1186/s12883-024-03989-2>.

Supplementary Material 1

Supplementary Material 2

Supplementary Material 3

Supplementary Material 4

## Acknowledgements

First of all, I would like to extend my sincere gratitude to my supervisor, Ying Zhou, for her instructive advice and useful suggestions on my thesis. I am deeply grateful of her help in completion of this thesis. I am also deeply indebted to all the other tutors and teachers in hospital for their direct and indirect help to me. Special thanks should go to my friends who have put considerable time and effort into their comments on the draft. Finally, I am indebted to my parents for their continuous support and encouragement. Zhen Yang was involved in the consultation and long-term follow-up of the patient, and was involved in the writing of the manuscript. Ying Zhou revised the manuscript and contributed to the completion of the manuscript. Li Liu was responsible for scale inspection. Tao You was responsible for statistical analysis. Lingling Wang, Fang Yi, Yu Jiang were responsible for fNIRS data collection. Thanks to all authors for their contributions to this article. The authors read and approved the final manuscript.

## Author contributions

Zhen Yang was involved in the consultation and long-term follow-up of the patient, and was involved in the writing of the manuscript. Ying Zhou revised the manuscript and contributed to the completion of the manuscript. Li Liu was responsible for scale inspection. Tao You was responsible for statistical analysis. Lingling Wang, Fang Yi, Yue Jiang were responsible for fNIRS data collection. All authors read and approved the final manuscript.

## Funding

The authors declare that they did not receive any funding from any source.

## Data availability

The data that support the findings of this study are available on request from the corresponding author.

## Declarations

### Ethics approval and consent to participate

This study followed the Declaration of Helsinki and received approval from the Ethics Committee of Changsha First Hospital on March 22, 2024. And all participants and legal guardians provides written informed consent.

### Consent for publication

N/A.

### Competing interests

The authors declare no competing interests.

### Author details

<sup>1</sup>Neurology Department, The First Affiliated Hospital of Shaoyang University, Shao Yang City 422000, China

<sup>2</sup>Neurology Department, The First Hospital of Chang Sha, Chang Sha City 410000, China

<sup>3</sup>Neurology Department, Zhuzhou Central Hospital, Zhuzhou City 412000, China

Received: 21 April 2024 / Accepted: 9 December 2024

Published online: 28 April 2025

## References

- Dubois B, Feldman HH, Jacova C, Hampel H, Molinuevo JL, Blennow K, DeKosky ST, Gauthier S, Selkoe D, Bateman R, Cappa S, Crutch S, Engelborghs S, Frisoni GB, Fox NC, Galasko D, Habert MO, Jicha GA, Nordberg A, Pasquier F, Rabinovici G, Robert P, Rowe C, Salloway S, Sarazin M, Epelbaum S, de Souza LC, Vellas B, Visser PJ, Schneider L, Stern Y, Scheltens P, Cummings JL. Advancing research diagnostic criteria for Alzheimer's disease: the IWG-2 criteria. *Lancet Neurol*. 2014;13(6):614–29. [https://doi.org/10.1016/S1474-4422\(14\)70090-0](https://doi.org/10.1016/S1474-4422(14)70090-0). Erratum in: *Lancet Neurol*. 2014;13(8):757. PMID: 24849862.
- Femminella GD, Thayanandan T, Calsolaro V, Komici K, Rengo G, Corbi G, Ferrara N. Imaging and molecular mechanisms of Alzheimer's disease: a review. *Int J Mol Sci*. 2018;19(12):3702. <https://doi.org/10.3390/ijms19123702>. PMID: 30469491; PMCID: PMC6321449.
- Iturria-Medina Y, Sotero RC, Toussaint PJ, Mateos-Pérez JM, Evans AC, Alzheimer's Disease Neuroimaging Initiative. Early role of vascular dysregulation on late-onset Alzheimer's disease based on multifactorial data-driven analysis. *Nat Commun*. 2016;7:11934. <https://doi.org/10.1038/ncomms11934>. PMID: 27327500; PMCID: PMC4919512.
- Iadecola C. The neurovascular unit coming of age: a journey through neurovascular coupling in Health and Disease. *Neuron*. 2017;96(1):17–42. <https://doi.org/10.1016/j.neuron.2017.07.030>. PMID: 28957666; PMCID: PMC5657612.
- Fisher RA, Miners JS, Love S. Pathological changes within the cerebral vasculature in Alzheimer's disease: New perspectives. *Brain Pathol*. 2022;32(6):e13061. doi: 10.1111/bpa.13061. Epub 2022 Mar 14. PMID: 35289012; PMCID: PMC9616094.
- Zhang F, Eckman C, Younkin S, Hsiao KK, Iadecola C. Increased susceptibility to ischemic brain damage in transgenic mice overexpressing the amyloid precursor protein. *J Neurosci*. 1997;17(20):7655–61. <https://doi.org/10.1523/JNEUROSCI.17-20-07655.1997>. PMID: 9315887; PMCID: PMC6793926.
- Niwa K, Carlson GA, Iadecola C. Exogenous A beta1-40 reproduces cerebrovascular alterations resulting from amyloid precursor protein overexpression in mice. *J Cereb Blood Flow Metab*. 2000;20(12):1659–68. <https://doi.org/10.1097/00004647-200012000-00005>. PMID: 11129782.
- Jalalvandi M, Riyahi Alam N, Sharini H, Hashemi H, Nadimi M, Brain Cortical Activation during Imagining of the Wrist Movement Using Functional Near-Infrared Spectroscopy (fNIRS), *Biomed Phys J Eng*, Jalalvandi M, Sharini H, Naderi Y, Riahi Alam N. Assessment of Brain Cortical Activation in Passive Movement during Wrist Task Using Functional Near Infrared Spectroscopy (fNIRS). *Frontiers Biomed Technol*. 2019;6(2):99–105. [46]H. Sharini, Fooladi M, Masjoodi S, Jalalvandi M. M. Yousef Pour, Identification of the Pain Process by Cold Stimulation: Using Dynamic Causal Modeling of Effective Connectivity in Functional Near-Infrared Spectroscopy (fNIRS), *IRBM*, Volume 40, Issue 2, 2019, Pages 86–94, ISSN 1959–0318, <https://doi.org/10.1016/j.irbm.2018.11.006>
- Chen WL, Wagner J, Heugel N, Sugar J, Lee YW, Conant L, Malloy M, Heffernan J, Quirk B, Zinos A, Beardsley SA, Prost R, Whelan HT. Functional Near-Infrared Spectroscopy and its clinical application in the field of Neuroscience: advances and future directions. *Front Neurosci*. 2020;14:724. <https://doi.org/10.3389/fnins.2020.00724>. PMID: 32742257; PMCID: PMC7364176.
- Drew PJ. Neurovascular coupling: motive unknown. *Trends Neurosci*. 2022;45(11):809–19. <https://doi.org/10.1016/j.tins.2022.08.004>. Epub 2022 Aug 19. PMID: 35995628; PMCID: PMC9768528.
- Chou PH, Huang CJ, Sun CW. The Potential Role of Functional Near-Infrared Spectroscopy as Clinical Biomarkers in Schizophrenia. *Curr Pharm Des*. 2020;26(2):201–217. <https://doi.org/10.2174/1381612825666191014164511>. PMID: 31612819.
- Cui X, Bray S, Bryant DM, Glover GH, Reiss AL. A quantitative comparison of NIRS and fMRI across multiple cognitive tasks. *NeuroImage*. 2011;54(4):2808–21. <https://doi.org/10.1016/j.neuroimage.2010.10.069>. Epub 2010 Nov 1. PMID: 21047559; PMCID: PMC3021967.
- Jöbsis FF. Noninvasive, infrared monitoring of cerebral and myocardial oxygen sufficiency and circulatory parameters. *Science*. 1977;198(4323):1264–7. <https://doi.org/10.1126/science.929199>. PMID: 929199.
- Wu H, Li T, Peng C, Yang C, Bian Y, Li X, Xiao Q, Wang P, Zhang Z, Zhang Y. The right prefrontal cortex (PFC) can distinguish anxious depression from non-anxious depression: a promising functional near infrared spectroscopy study (fNIRS). *J Affect Disord*. 2022;317:319–28. Epub 2022 Aug 22. PMID: 36007594.
- Nguyen T, Kim M, Gwak J, Lee JJ, Choi KY, Lee KH, Kim JG. Investigation of brain functional connectivity in patients with mild cognitive impairment: a functional near-infrared spectroscopy (fNIRS) study. *J Biophotonics*. 2019;12(9):e201800298. <https://doi.org/10.1002/jbio.201800298>. Epub 2019 May 17. PMID: 30963713.
- Tang TB, Chan YL. Functional Connectivity Analysis on Mild Alzheimer's Disease, Mild Cognitive Impairment and Normal Aging using fNIRS. *Annu Int Conf IEEE Eng Med Biol Soc*. 2018;2018:17–20. <https://doi.org/10.1109/EMBC.2018.8512186>. PMID: 30440330.
- Hiraoka M, Firbank M, Essenpreis M, Cope M, Arridge SR, van der Zee P, Delpy DT. A Monte Carlo investigation of optical pathlength in inhomogeneous tissue and its application to near-infrared spectroscopy. *Phys Med Biol*. 1993;38(12):1859–76. <https://doi.org/10.1088/0031-9155/38/12/011>. PMID: 8108489.
- Hong KS, Khan MJ, Hong MJ. Feature extraction and classification methods for hybrid fNIRS-EEG brain-computer interfaces. *Front Hum Neurosci*. 2018;12:246. <https://doi.org/10.3389/fnhum.2018.00246>. PMID: 30002623; PMCID: PMC6032997.
- Yang D, Huang R, Yoo SH, Shin MJ, Yoon JA, Shin YI, Hong KS. Detection of mild cognitive impairment using convolutional neural network: temporal-feature maps of Functional Near-Infrared Spectroscopy. *Front Aging Neurosci*. 2020;12:141. <https://doi.org/10.3389/fnagi.2020.00141>. PMID: 32508627; PMCID: PMC7253632.
- Ohshima S, Koeda M, Kawai W, Saito H, Nioka K, Okuno K, Naganawa S, Hama T, Kyutoku Y, Dan I. Cerebral response to emotional working memory based on vocal cues: an fNIRS study. *Front Hum Neurosci*. 2023;17:1160392. <https://doi.org/10.3389/fnhum.2023.1160392>. PMID: 38222093; PMCID: PMC10785654.
- Stuart S, Vitorio R, Morris R, Martini DN, Fino PC, Mancini M. Cortical activity during walking and balance tasks in older adults and in people with Parkinson's disease: a structured review. *Maturitas*. 2018;113:53–72. <https://doi.org/10.1016/j.maturitas.2018.04.011>. Epub 2018 Apr 25. PMID: 29903649; PMCID: PMC6448561.
- Tak S, Kempny AM, Friston KJ, Leff AP, Penny WD. Dynamic causal modelling for functional near-infrared spectroscopy. *NeuroImage*. 2015;111:338–49. <https://doi.org/10.1016/j.neuroimage.2015.02.035>. Epub 2015 Feb 25. PMID: 25724757; PMCID: PMC4401444.
- Hou X, Zhang Z, Zhao C, Duan L, Gong Y, Li Z, Zhu C. NIRS-KIT: a MATLAB toolbox for both resting-state and task fNIRS data analysis. *Neurophotonics*. 2021;8(1):010802. <https://doi.org/10.1117/1.NPh.8.1.010802>. Epub 2021 Jan 25. PMID: 33506071; PMCID: PMC7829673.
- Xia M, Wang J, He Y. BrainNet Viewer: a network visualization tool for human brain connectomics. *PLoS One*. 2013;8(7):e68910. <https://doi.org/10.1371/journal.pone.0068910>. PMID: 23861951; PMCID: PMC3701683.
- Rofes A, de Aguiar V, Jonkers R, Oh SJ, DeDe G, Sung JE. What drives Task Performance during Animal Fluency in People with Alzheimer's Disease? *Front Psychol*. 2020;11:1485. <https://doi.org/10.3389/fpsyg.2020.01485>. PMID: 32774312; PMCID: PMC7388773.
- Aita SL, Beach JD, Taylor SE, Borgogna NC, Harrell MN, Hill BD. Executive, language, or both? An examination of the construct validity of verbal fluency measures. *Appl Neuropsychol Adult*. 2019 Sep–Oct;26(5):441–51. Epub 2018 Mar 7. PMID: 29513079.
- Wright LM, De Marco M, Venneri A. Current understanding of Verbal Fluency in Alzheimer's Disease: evidence to date. *Psychol Res Behav Manag*. 2023;16:1691–705. <https://doi.org/10.2147/PRBM.S284645>. PMID: 37179686; PMCID: PMC10167999.
- Viena TD, Rasch GE, Silva D, Allen TA. Calretinin and calbindin architecture of the midline thalamus associated with prefrontal-hippocampal circuitry. *Hippocampus*. 2021;31(7):770–89. <https://doi.org/10.1002/hipo.23271>. Epub 2020 Oct 21. PMID: 33085824; PMCID: PMC8805340.
- von Halbach BU, Draguhn O, Storm-Mathisen A. J. Recent advances in hippocampal structure and function. *Cell Tissue Res*. 2018;373(3):521–523. <https://doi.org/10.1007/s00441-018-2913-z>. PMID: 30128595.
- Uemura K, Shimada H, Doi T, Makizako H, Tsutsumimoto K, Park H, Suzuki T. Reduced prefrontal oxygenation in mild cognitive impairment during

- memory retrieval. *Int J Geriatr Psychiatry*. 2016;31(6):583–91. <https://doi.org/10.1002/gps.4363>. Epub 2015 Sep 21. PMID: 26387497.
31. Yap KH, Ung WC, Ebenezer EGM, Nordin N, Chin PS, Sugathan S, Chan SC, Yip HL, Kiguchi M, Tang TB. Visualizing hyperactivation in Neurodegeneration based on Prefrontal Oxygenation: a comparative study of mild Alzheimer's disease, mild cognitive impairment, and Healthy Controls. *Front Aging Neurosci*. 2017;9:287. <https://doi.org/10.3389/fnagi.2017.00287>. PMID: 28919856; PMCID: PMC5585736.
  32. Park DC, Bischof GN. The aging mind: neuroplasticity in response to cognitive training. *Dialogues Clin Neurosci*. 2013;15(1):109–19. <https://doi.org/10.31887/DCNS.2013.15.1/dpark>. PMID: 23576894; PMCID: PMC3622463.
  33. Smith SM, Fox PT, Miller KL, Glahn DC, Fox PM, Mackay CE, Filippini N, Watkins KE, Toro R, Laird AR, Beckmann CF. Correspondence of the brain's functional architecture during activation and rest. *Proc Natl Acad Sci U S A*. 2009;106(31):13040–5. <https://doi.org/10.1073/pnas.0905267106>. Epub 2009 Jul 20. PMID: 19620724; PMCID: PMC2722273.
  34. O'Donnell C, van Rossum MC. Systematic analysis of the contributions of stochastic voltage gated channels to neuronal noise. *Front Comput Neurosci*. 2014;8:105. <https://doi.org/10.3389/fncom.2014.00105>. PMID: 25360105; PMCID: PMC4199219.
  35. Koychev I, Hofer M, Friedman N. Correlation of Alzheimer Disease Neuro-pathologic staging with amyloid and tau scintigraphic imaging biomarkers. *J Nucl Med*. 2020;61(10):1413–8. <https://doi.org/10.2967/jnumed.119.230458>. Epub 2020 Aug 6. PMID: 32764121.
  36. Skoog I. The relationship between blood pressure and dementia: a review. *Biomed Pharmacother*. 1997;51(9):367–75. [https://doi.org/10.1016/s0753-3322\(97\)89428-0](https://doi.org/10.1016/s0753-3322(97)89428-0). PMID: 9452785.
  37. Janota C, Lemere CA, Brito MA. Dissecting the contribution of vascular alterations and aging to Alzheimer's disease. *Mol Neurobiol*. 2016;53(6):3793–3811. <https://doi.org/10.1007/s12035-015-9319-7>. Epub 2015 Jul 5. PMID: 26143259.
  38. Toledo JB, Arnold SE, Raible K, Brettschneider J, Xie SX, Grossman M, Monsell SE, Kukull WA, Trojanowski JQ. Contribution of cerebrovascular disease in autopsy confirmed neurodegenerative disease cases in the National Alzheimer's coordinating centre. *Brain*. 2013;136(Pt 9):2697–706. <https://doi.org/10.1093/brain/awt188>. Epub 2013 Jul 10. PMID: 23842566; PMCID: PMC3858112.
  39. Dubois B, Feldman HH, Jacova C, Cummings JL, Dekosky ST, Barberger-Gateau P, Delacourte A, Frisoni G, Fox NC, Galasko D, Gauthier S, Hampel H, Jicha GA, Meguro K, O'Brien J, Pasquier F, Robert P, Rossor M, Salloway S, Sarazin M, de Souza LC, Stern Y, Visser PJ, Scheltens P. Revising the definition of Alzheimer's disease: a new lexicon. *Lancet Neurol*. 2010;9(11):1118–27. [https://doi.org/10.1016/S1474-4422\(10\)70223-4](https://doi.org/10.1016/S1474-4422(10)70223-4). Epub 2010 Oct 9. PMID: 20934914.
  40. Kolk SM, Rakic P. Development of prefrontal cortex. *Neuropsychopharmacology*. 2022;47(1):41–57. <https://doi.org/10.1038/s41386-021-01137-9>. Epub 2021 Oct 13. PMID: 34645980; PMCID: PMC8511863.
  41. Guse B, Falkai P, Wobrock T. Cognitive effects of high-frequency repetitive transcranial magnetic stimulation: a systematic review. *J Neural Transm (Vienna)*. 2010;117(1):105–22. doi: 10.1007/s00702-009-0333-7. Epub 2009 Oct 27. PMID: 19859782; PMCID: PMC3085788.
  42. Saita K, Morishita T, Arima H, Hyakutake K, Ogata T, Yagi K, Shiota E, Inoue T. Biofeedback effect of hybrid assistive limb in stroke rehabilitation: a proof of concept study using functional near infrared spectroscopy. *PLoS ONE*. 2018;13(1):e0191361. <https://doi.org/10.1371/journal.pone.0191361>. PMID: 29338060; PMCID: PMC5770063.

### Publisher's note

Springer Nature remains neutral with regard to jurisdictional claims in published maps and institutional affiliations.